CS660 - Final Report
Applying Mamba to GNNs

Jyotirmaya Shivottam
23226001
School of Computer Science
National Institute of Science Education and Research
Bhubaneswar, Odisha
`jyotirmaya.shivottam@niser.ac.in`

Abstract

In this report, we present the work done towards the semester project for the CS660 - Machine Learning course. As mentioned in our proposal[1], we attempted to combine the efficiency and effectiveness of a novel Structured State Space Model, called "*Mamba*" [1] on long-range sequence modeling, with message-passing graph neural networks. We did so by devising a new state update method for the embeddings of the graph nodes. In the midway submission[2], we reported our results on the Planetoid [2] dataset, along with several ablation experiments that revealed some interesting issues with our approach. In particular, we faced issues with deeper models and ineffectiveness of Mamba on static graphs. In this project update, we conduct more experiments on static graphs, specifically to test the viability of deeper models, alongside extending the approach to work on spatio-temporal or dynamic graphs. We discuss the model's performance on dynamic graphs and outline future work.

1 Introduction

1.1 A Refresher on Graph Neural Networks

We begin by reviewing the basics of GNNs, particularly Message Passing Neural Networks (MPNNs) [3]. First, let us introduce the mathematical notation we use throughout this work. Let $\mathcal{G} = (\mathcal{V}, \mathcal{E})$ denote a graph with vertex (node) set, $\mathcal{V}$ and edge set, $\mathcal{E}$. Let $N = |\mathcal{V}|$. For simplicity, we assume that the graph is undirected and unweighted, but the methods we discuss in this report are easily extensible to directed and weighted graphs. We use $\mathcal{N}[i]$ to represent the closed set of neighbors of node i. Moreover, let $X \in \mathbb{R}^{N \times F}$ be the node feature matrix, where F is the number of features per node, i.e., $X = [x_1, x_2, \dots, x_N]^T$, where $x_i \in \mathbb{R}^F$. It should be noted that, in set notation, X and intermediate feature maps are multisets, as two nodes can have identical features. We use $A \in \mathbb{R}^{N \times N}$ to denote the graph's adjacency matrix.

Message Passing Neural Networks (MPNNs) MPNNs are a class of GNNs that aggregate & update node features based on the features of their neighbors. The following set of iterative steps

[1]Group 0 – Proposal – `https://t.ly/m7GuB`
[2]Group 0 – Midway Report – `https://t.ly/Tzq42`

Preprint. Under review.

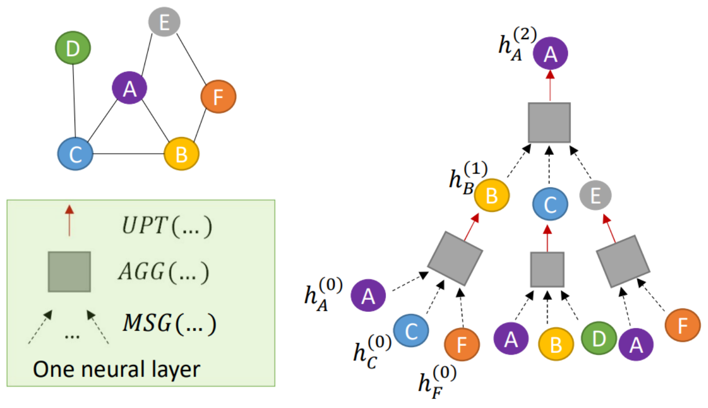

Figure 1: Application of a Message-Passing GNN layer, shown for one node (Taken from [4])

defines these models:

$$m_i^{(l)} = \texttt{MESSAGE}\left(\{h_j^{(l-1)} : j \in \mathcal{N}[i]\}\right) \tag{1}$$

$$a_i^{(l)} = \texttt{AGGREGATE}\left(\{m_j^{(l-1)} : j \in \mathcal{N}[i]\}\right) \tag{2}$$

$$h_i^{(l)} = \texttt{UPDATE}\left(h_i^{(l-1)}, a_i^{(l)}\right) \tag{3}$$

Here, l denotes a particular GNN layer, $h_i^{(l)}$ is the hidden state of node i at layer l, $m_i^{(l)}$ is the "message" generated for node i using the hidden states at layer l, and $a_i^{(l)}$ denotes the aggregated message for node i at layer l. The functions MESSAGE, AGGREGATE, and UPDATE are typically parameterized by neural network layers, such as multi-layer perceptrons (MLPs) and are shared across all nodes in the graph. Figure 1 illustrates these. The final output is obtained by applying a READOUT function to the final hidden states, i.e., $O = \texttt{READOUT}(\{h_i^{(L)} : i \in [N]\})$, where L is the number of layers in the GNN, at either node or graph level, depending on the task at hand, which can be node classification, graph classification, etc.

Since graph data is naturally unordered [5], i.e., the elements of $\mathcal{V}$ are unordered, the neural network layers representing the functions mentioned above that operate on node features must be permutation-invariant [5]. In fact, the primary reason to learn on graphs is the inductive bias or symmetry that graph data is inherently order-independent. As such, MPNNs usually enforce that AGGREGATE remains permutation-invariant by using functions such as sum, mean, or max for fixed (unlearned) aggregation or by combining these with learned weights.

1.2 Related Works

In practice, different MPNN variants, such as Graph Convolution (GCN) [6], Gated Graph Convolution (GGSNN) [7], GraphSAGE [8] and Graph Attention (GAT) [9, 10] or Graph Transformers [11], differ mainly in the way they define the functions – MESSAGE, AGGREGATE, and UPDATE, and hence, in the way they collect and update the node features. For instance, GCN updates node features via a first-order approximation of spectral graph convolutions in a way quite similar to fixed image convolution kernels; GGSNN uses the Gated Recurrent Unit update for node features, followed by a neighbourhood sum aggregation, while GraphSAGE trains a set of aggregator functions operating on different hops on sampled node neighbourhoods. In contrast, Graph Attention (GAT) uses a self-attention mechanism on node neighborhoods with sum aggregation.

As discussed by Xu et al. [12], all of the aforementioned models are at most as expressive as the 1-Weisfeiler-Lehman (1-WL) graph isomorphism test. This becomes particularly problematic for graph data with long-range dependencies, e.g., in many real-world applications, such as social network analysis, recommendation systems, bioinformatics, or when learning on heterophilic graphs. Moreover, approaches like GAT or Graph Transformers, which can technically model long-range dependencies as long as multi-hop neighborhoods are considered, are hampered by the $\mathcal{O}(N^2)$

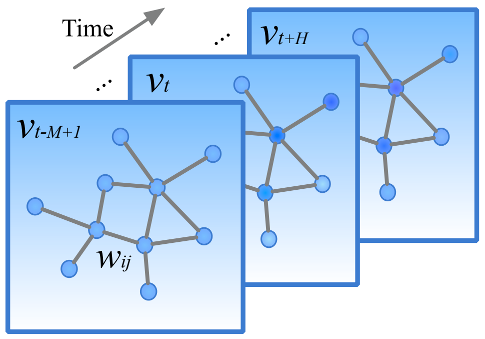

Figure 2: A dynamic (spatio-temporal) graph with node features changing with time (Taken from [13])

complexity scaling of the attention mechanism, which makes them infeasible for large graphs. In particular, Graph Transformers treat graphs as a sequence of nodes, much like sequences of tokens in natural language processing, and process nodes within pre-defined context windows. To mitigate the quadratic complexity of attention, they usually perform ‘attention sparsification’, where nodes are subsampled prior to computing attention scores.

Message Passing Graph Neural Networks (GNNs) have also been extended to dynamic or spatio-temporal graphs. In these cases, the graph-structured data includes a temporal dimension with changing node and/or edge features over time (Fig. 2). Extending MPNNs to such scenarios typically involves utilizing architectures like GCN for spatial dependencies and flavours of sequence modeling networks like Recurrent Neural Networks (RNNs), such as Gated Recurrent Unit (GRU) or Gated Linear Unit (GLU), for inter-graph temporal dependencies. For instance, the Diffusion Convolutional Recurrent Neural Network (DCRNN) [14] utilizes GCN for spatial convolution and RNNs for temporal dependencies. Other methods like Spatio-Temporal Graph Convolutional Networks (STGCN) [13] and Graph WaveNet (GWN) [15] combine graph convolutions with (dilated) causal convolutions to extract spatial-temporal dependencies simultaneously. Spatial-Temporal Synchronous GCNs (STSGCN) [16] capture localized spatial-temporal correlations synchronously by treating small batches of graph-states and employing message-passing between nodes across time-steps. Adaptive Graph Convolutional Recurrent Network (AGCRN) [17] handles edge features via adaptive parameter learning and models the sequence of graph-states using the GRU mechanism. Spatio-Temporal Wavelet NN (STWave) [18] introduces a disentangle-fusion framework to address distribution shift, decoupling traffic data into stable trends and fluctuating events modeled by a dual-channel spatio-temporal network. It incorporates novel query sampling and graph wavelet-based positional encoding into an attention-sparsified spectral graph attention network for efficient dynamic spatial correlation modeling. Spatio-Temporal Adaptive Embedding Transformer (STAEformer) [19] focuses on generating input embeddings for feature modalities and fusing them prior to passing through temporal and spatial transformer blocks. While not explicitly a graph-based approach, STAEformer is the current state-of-the-art on several traffic forecasting graph datasets.

It is clear that there is a trend here of using MPNNs to model the spatial dependencies, while leveraging some form of a *seq2seq* model to handle the temporal behaviour. Mamba, being an SSM (very similar to an RNN), is well-suited to such a task. Additionally, it has proven to be capable of handling long-range dependencies without many of the downsides of RNNs. In the next sections, we discuss Mamba, a new time-varying state-space model proposed recently by Gu et al. [1], that comes equipped with a ‘selection’ mechanism, that scales linearly with sequence length and how we can adapt it for MPNNs.

2 Selective State Space-based Sequence Modeling via Mamba

Recently, Gu et al. [1] proposed a novel sequence modeling framework, based on structured state space models (SSM), with a selection mechanism, called *Mamba*, that is capable of learning long-range dependencies in sequential data in an input-dependent manner. SSMs relate a continuous input sequence, $x(t) \in \mathbb{R}$, to a continuous output sequence, $y(t) \in \mathbb{R}$, through an implicit latent state,

$h(t) \in \mathbb{R}^d$, using the following first-order ordinary differential equation:

$$h'(t) = Ah(t) + Bx(t) \tag{4}$$

$$y(t) = Ch(t) + Dx(t) \tag{5}$$

Here, $A \in \mathbb{R}^{d\times d}$, $B \in \mathbb{R}^{d\times 1}$, $C \in \mathbb{R}^{1\times d}$, and $D \in \mathbb{R}$ are the state transition matrix, the input matrix, the output matrix, and the feedforward matrix, respectively. We omit D going forward, as it is usually modeled as a skip connection. As we work with discrete data, these equations, and hence, the associated parameters, are discretized using Zero-Order Hold (ZOH) to obtain the following update (recurrence) equations:

$$\bar{A} \overset{\text{ZOH}}{:=} \exp(\Delta A) \tag{6}$$

$$\bar{B} \overset{\text{ZOH}}{:=} (\Delta A)^{-1}(\exp(\Delta A) - \mathbb{I}) \cdot \Delta B \tag{7}$$

$$h_t = \bar{A}h_{t-1} + \bar{B}x_t \tag{8}$$

$$y_t = Ch_t \tag{9}$$

Here, $x_t, y_t \in \mathbb{R}^F$, the subscript, t, is the time step along the sequence, and Δ denotes a learned (adaptive) discretization step size. In contrast with prior SSM architectures, in Mamba, the Δ parameter is made input-dependent, which indirectly makes A, B & C input-dependent, using the following learned projections:

$$B \leftarrow s_B(x) = \texttt{Linear}_N(x) \tag{10}$$

$$C \leftarrow s_C(x) = \texttt{Linear}_N(x) \tag{11}$$

$$s_\Delta(x) \leftarrow \texttt{Broadcast}_D(\texttt{Linear}(x)) \tag{12}$$

$$\Delta \leftarrow \texttt{softplus}(\texttt{Parameter} + s_\Delta(x)) \tag{13}$$

$$\bar{A}, \bar{B} \leftarrow \texttt{ZOH}(\Delta, A, B) \tag{14}$$

These specific choices have been made due to a connection to the RNN gating mechanism for particular s_Δ and τ_Δ (cf. Theorem 1 in [1]). Here, Δ acts as a **gating**, or what the Mamba authors term as a **selection** mechanism, that decides which parts of the input and the latent space are relevant to the current output, and hence, imparts shift-variant context-awareness to the Mamba block, allowing it to focus on or filter out different aspects or features of the input sequence, thereby, learning time-varying long-range dynamics. In addition, the state transition matrix, A, is "structured" as a diagonal matrix to stabilize the state update over long sequences and simplify the computation, because a diagonal A makes the discretization (exponentiation) trivial to calculate. Several fixed initializations exist for A. They are reasoned via the HiPPO theory [20], which allows these structured SSMs to memorize the input history in a controlled manner. The latent state, $h(t)$, is responsible for storing "compressed context" (h is d-dimensional, where $d \ll L$, the sequence length), as opposed to a transformer's full uncompressed context, which leads to Mamba's high efficiency. In general, Mamba's computational complexity only scales as $\mathcal{O}(L)$ as opposed to $\mathcal{O}(L^2)$ for transformer-based approaches. Finally, a clever hardware-aware implementation of an associative scan algorithm for the recurrence enables efficient training on modern hardware, making Mamba a practical choice for sequence modeling tasks. Figure 3 depicts a typical Mamba block, where the input is linearly projected ("state expansion") before passing through a short 1D depth-wise convolution and the main SSM update, with interleaved non-linearities. The final output of the block is a deflating linear projection. The structure of this block is inspired by the vanilla transformer and its simplifications used in prior SSM architectures (See the discussion in [1]).

3 Our Approach – Expressive Graph Mamba (EGM)

In this section, we describe how we integrate the Mamba block into a GNN to obtain what we call the "Expressive Graph Mamba" (EGM) layer, based on the discussion in previous sections, particularly on Mamba in Section 2. Now, let us delineate our Expressive Graph Mamba layer. Like other MPNN variants, we redefine one of the MPNN iterative steps – `UPDATE`. We start by considering a sequence of graph representations at different time steps, i.e., $X^0, X^1, \ldots, X^L$, where $X^0 = X$ is the initial node feature matrix, and L is the number of time steps (a hyperparameter). If edge attributes are present, they can be easily added to either X or the adjacency matrix, A. We use a shared Mamba

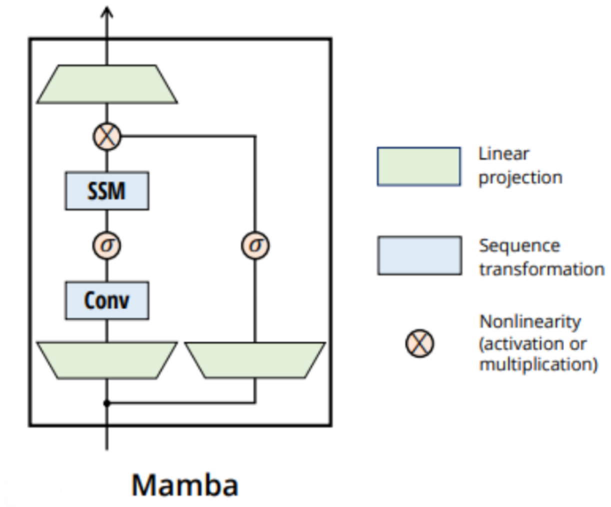

Figure 3: A Mamba Block [1] with state expansion (`Linear`$(\cdot)$)

block to update the node features at each time step, thereby leveraging the selection mechanism to allow the model to self-select the relevant aspects of the node features. Node features at time step 0, i.e., $X^0 = [x_1^0, \dots, x_N^0]^T$ form the input to our model. Then, for each node, $x_i \in \mathbb{R}^F$ (where F is the number of features per node), we proceed as follows:

`UPDATE` via `Mamba` block:

$$h_i^{(t+1)} = \bar{A}h_i^t + \bar{B}x_i^t \tag{15}$$

$$y_i^{(t+1)} = Ch_i^t \tag{16}$$

Here, $h \in \mathbb{R}^d$, where d denotes the model dimension, and $y \in \mathbb{R}^F$ is the output of the Mamba block. The parameters, $\bar{A}, \bar{B}, C$, are shared across all nodes in the graph and are learned during training (via the discretization, Δ, for $\bar{A}$ and $\bar{B}$). Here, we can choose to evolve the hidden states for a fixed number of time steps, say T, before passing the output to the following `AGGREGATE` step. This can be understood as a form of warmup for the Mamba block, similar to warmup for certain RNN or attention-based models.

The aggregation of node features in our case can be learned or fixed, e.g., using the usual sum, max, or mean aggregation. For learned aggregation, we combine the Mamba update with a shared attention mechanism, in the same vein as GAT or GATv2 [9, 10], reinforcing the model's ability to capture long-range dependencies in graph-structured data.

`AGGREGATE` via shared attention

$$\alpha_{ij} = \frac{\exp\left[\sigma\left(\vec{a}^{(t+1)T}\left[W^{(t+1)}y_i^{(t+1)}||W^{(t+1)}y_j^{(t+1)}\right]\right)\right]}{\sum_{k\in\mathcal{N}[i]}\exp\left[\sigma\left(\vec{a}^{(t+1)T}\left[W^{(t+1)}y_i^{(t+1)}||W^{(t+1)}y_k^{(t+1)}\right]\right)\right]} \tag{17}$$

$$x_i^{(t+1)} := y_i^{(t+1)} = \rho\left(\sum_{j\in\mathcal{N}[j]}\alpha_{ij}W^{(t+1)}y_j^{(t+1)}\right) \tag{18}$$

Here, $W^{(t+1)} \in \mathbb{R}^{F\times F}$ is a shared weight matrix, which transforms the output of the Mamba block; $\vec{a}^{(t+1)} \in \mathbb{R}^{2F}$ is a weight vector characterizing a single-layer feedforward NN, while σ and ρ are non-linearities. Furthermore, $(\cdot)^T$ denotes transposition, while $||$ represents concatenation. Since the Mamba block already calculates linear projections of the input features via state-expansion, W can be optional, as $\vec{a}$ alone should be sufficient for adding learnability to the computation of the attention coefficients. For this report, however, we utilize the entire GAT block.

Our goal here is to use the attention mechanism to aggregate the node features, while the SSM dynamics handles the latent space updates. One can relate this to the MPNN steps listed in Section 1.1

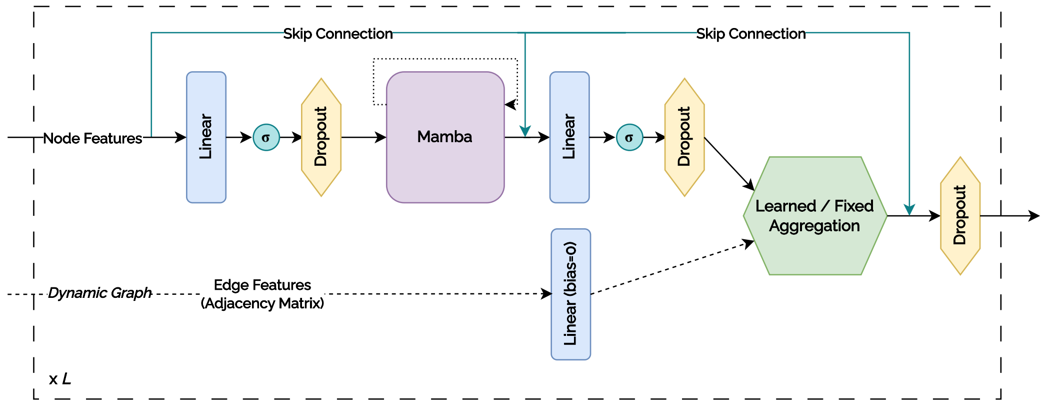

Figure 4: An (ST)EGM Block. Here, σ denotes SiLU non-linearity, while the aggregation can be fixed (sum, max, mean) or learned. L designates the number of EGM blocks or layers. The edge features are passed through a bias-free `Linear` layer for dynamic graphs.

Table 1: Dataset Information (Static graphs)

Name	#nodes	#edges	#features	#classes
Cora	2,708	10,556	1,433	7
CiteSeer	3,327	9,104	3,703	6
PubMed	19,717	88,648	500	3

– message generation, aggregation, and update, (Eqs. 1, 2, and 3). The SSM dynamics combines the message generation and update steps, while the shared attention mechanism combines the update and aggregation steps. After evolving the graph for L time steps, we obtain the final graph representation, $X^L = [x_1^L, \dots, x_N^L]^T$, which can be used for various downstream tasks. Similar to MPNNs, we use a learned `READOUT` to obtain the final output, $O = \texttt{READOUT}(X^L)$, via a single `Linear` layer. To extend this model to dynamic or spatio-temporal graphs, we apply a bias-free `Linear` layer to the edge-feature-weighted adjacency matrix of the graph (cf. Node Adaptive Parameter Learning from AGCRN). We expect that the effectiveness of Mamba as a long-range *seq2seq* block will enable EGM to model temporal dependencies in dynamic graphs.

Figure 4 shows a single (ST)EGM block. It can be stacked analogously to other MPNN blocks like GCN to allow information flow between multi-hop neighbourhoods. The following section describes the experiments performed using the (ST)EGM layers and discusses the corresponding results.

4 Experiments & Results

Due to time constraints for this report, we test the effectiveness of our approach on only the Planetoid (Cora, Citeseer, and Pubmed) datasets [2], that comprise citation networks in various domains, with the nodes in the graphs representing academic documents and the edges characterizing citation links, for the static case. For the dynamic graph setting, we evaluate the model on a real world dataset provided by the California Transportation Agencies (CalTrans) Performance Measurement System (PeMS) – PeMS08. PeMS08 is a collection of *traffic flow* measurements taken between July and August 2016 from 170 loop detector sensors placed on 8 roads in California. In total, there are 17,856 snapshots, at 5-minute intervals. The task is to forecast traffic flow 12-steps (or, 1 hour) into the future. The edge features in the 170-node sensor graph are formed using pairwise road network distances between the sensors [14]. We used the Planetoid dataset class from PyTorch Geometric[3] to load the data, as it comes with pre-made binary masks for the training, validation, and tests splits. Table 1 summarizes the details of the Planetoid datasets. These datasets are relatively fast to train on, enabling us to iterate on the design of our network architecture at a fast rate.

[3]`https://pytorch-geometric.readthedocs.io/en/latest/`

Table 2: Training Information. (*) indicates the best-performing component.

Loss Function	`CrossEntropy`
(ST)EGM Loss Function(s)	`MSELoss`, `MAELoss`, `RMSELoss`, `HuberLoss` (*)
Scheduler	`ExponentialLR` (*), `LambdaLR` (*), `LinearLR`, `OneCycleLR`
Optimizer	`RAdam` (*), `Adam` (*), `AdamW`
Weight Decay	0.0005
Learning Rate	$[0.0001, 0.01]$
EGM Layers	$\{1, 2, 3, 4, 6, 8\}$
(ST)EGM Layers	$\{1, 2, 3, 4, 6\}$
Epochs	$[50, 500]$

The previously mentioned MPNN models – GCN, GAT, GATv2, GraphSAGE, and GIN, serve as the baselines for comparison in the static case. Specifically, we train all these models for the node classification task. For the dynamic case, we compare against published results for the aforementioned models – DCRNN, STGCN, GWNet, STSGCN, AGCRN, STAEformer and STWave, as reported by the authors of the STAEformer and STWave papers.

As depicted in Fig. 4, we use interleaved skip connections, SiLU activation, and dropout layers to facilitate stable training for our EGM model. To further stabilize training, we use Layer Normalization [21] between the EGM layers. Here, the Mamba block is taken from the mamba-ssm[4] Python library by the original Mamba authors. The rest of the model has been implemented from scratch in PyTorch[5] and PyTorch Geometric. Table 2 outlines the remaining training-related information. We use `CrossEntropy` as the loss function for the static graphs, as the task is multi-class node classification, while we trialed several loss functions for the dynamic graph forecasting task, ultimately finding `HuberLoss` [22], which is a smoothed, thresholded version of mean absolute error, to be the best performing. Note that we use the `RAdam` optimizer instead of `Adam` or `AdamW`, as `RAdam` constrains the variance of the adaptive learning rate during the early stages of the training [23], which leads to more stable training during the initial epochs in our experiments.

We experiment with different numbers of EGM layers, but for every comparison, we maintain a similar structure for all the models with an unconstrained parameter budget. Note that, due to time limitations, no hyperparameter search was performed for any of the models. Each experiment was run with 3 - 5 different seeds (depending on dataset-dependent VRAM requirement), and the mean and standard deviation of the test accuracy were computed. In total, roughly 600 experiments were conducted and tracked on WandB[6][7], resulting in a total of 1,743 runs. In the next section, we compare against the aforementioned baselines and discuss the results of this work.

5 Results & Discussion

In this section, we present the results of the experiments conducted using our approach on the Planetoid and PEMS08 datasets.

The performance plots depicted in Fig. 5 demonstrate that EGM achieves comparable results to other MPNN baselines on static graph datasets. Its performance falls within the standard deviation range of other models across all datasets we could test. Interestingly, we observe that employing fixed aggregation functions, such as `mean`, `sum`, and particularly `max`, yields superior results compared to learned aggregation schemes that integrate message-passing. This observation is illustrated in Figure 6(a). Additionally, this suggests that the previously proposed GAT-based aggregation method may not be suitable for our model. A probable cause here could be the potential over-smoothing of node features, as the learned aggregators in our setup incorporate their own aggregation schemes, except for simpler aggregators like GIN or GCN. Furthermore, as depicted in Fig. 6(b), the accuracy

[4]`https://github.com/state-spaces/mamba`

[5]`https://pytorch.org/`

[6]`https://wandb.ai/js-exps/graphmamba`

[7]`https://wandb.ai/js-exps/stgraphmamba`

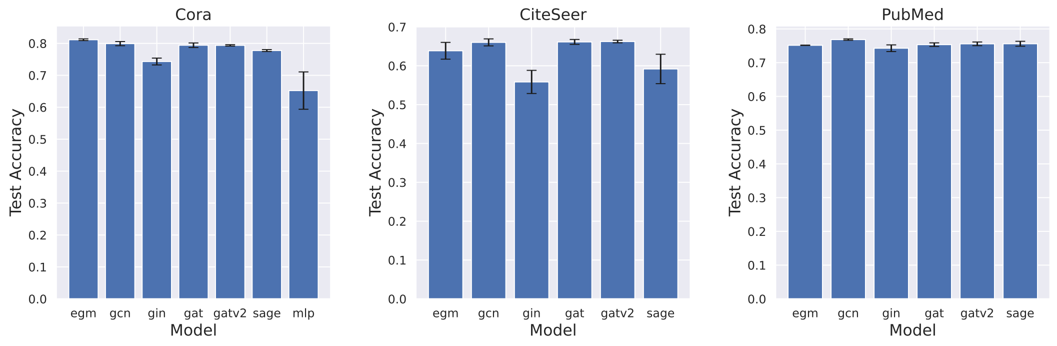

Figure 5: Performance comparison of our model (EGM) with baselines on the Planetoid datasets. Here, `mlp` is a simple multi-layer perception model with sum aggregation.

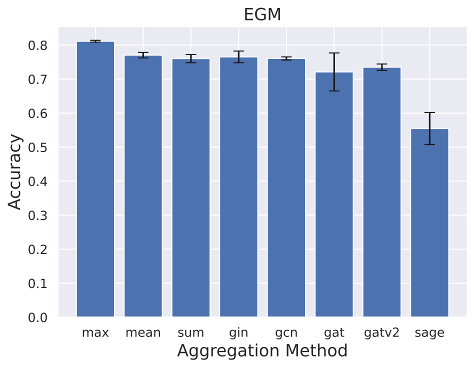

(a) Testing different fixed aggregation schemes for EGM. Surprisingly, fixed aggregation performs better than learned.

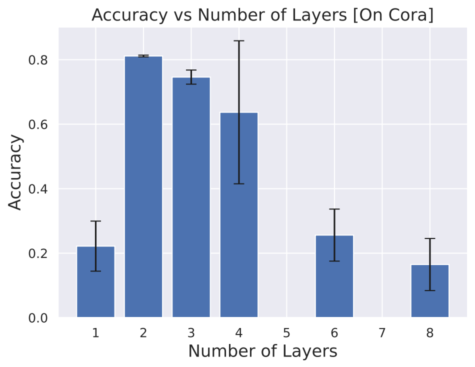

(b) Model accuracy drops drastically with increasing variance, as the number of EGM layers increases. No tests were done for layer count = 5 and 7.

Figure 6: Different experiments performed on the EGM architecture

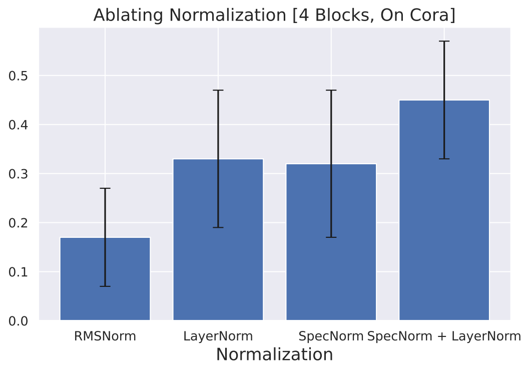

(a) For 4 blocks, a mixture of LayerNorm and SpectralNorm performs the best.

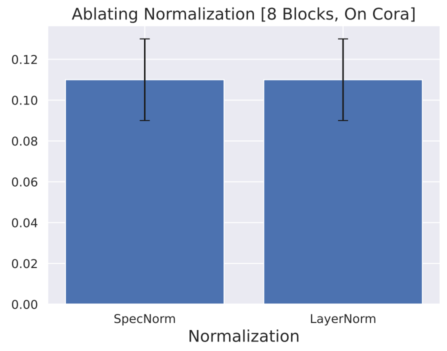

(b) For 8 blocks, there is negligible difference between the two normalizations.

Figure 7: Effect of various normalization schemes on the EGM architecture

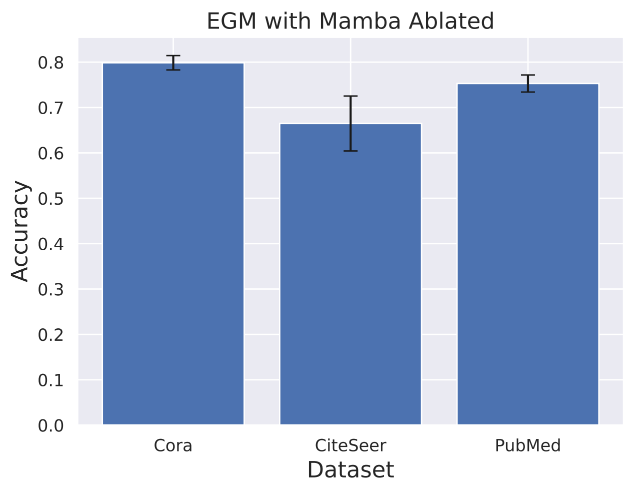

Figure 8: Accuracy scores after ablating the Mamba block from the EGM block. Unexpectedly, the performance without Mamba is comparable to the complete EGM architecture (cf. Figure 5).

Table 3: Performance on PEMS08 (Baselines reported via STAEformer [19] & STWave [18])

Metric	MAE	RMSE	MAPE
DCRNN	15.22	24.17	10.21%
STGCN	16.08	25.39	10.60%
GWNet	14.40	23.39	9.21%
STSGCN	17.13	26.80	10.96%
AGCRN	15.32	24.41	10.03%
STWave	**13.42**	23.40	8.90%
STAEformer	13.46	**23.25**	**8.88%**
STEGM (**Untuned**)	21.44	33.09	13.62%

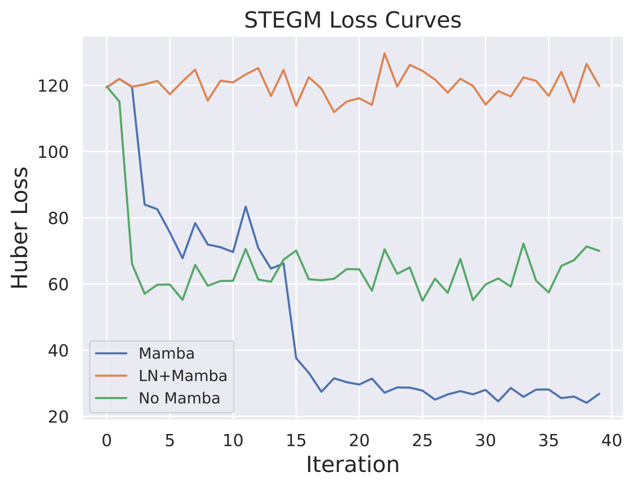

Figure 9: Loss curves after ablating different parts of the STEGM block. In particular, note the better training with the Mamba block present.

of our model notably decreases as the number of layers increases. While over-smoothing may contribute to this phenomenon too, we also observed large activations in the Mamba block beyond a certain number of layers (> 3), suggesting that the Mamba block struggles to learn stably. This is at odds with Graph Transformer networks, which can effectively learn on graphs (albeit when nodes are treated sequentially) with as many as six layers [11]. To further analyze this, we explored the potential of more sophisticated normalization schemes, such as RMS Layer Normalization [24] and Spectral Normalization [25], that should, in principle, stabilize the training by rescaling the impact of large activations on weight updates. However, as depicted in Fig. 7, the rescaling does not have an impact on the performance drop-off, especially for deeper models ($L > 4$).

Importantly, we made an intriguing observation during ablative experiments on the Mamba block. As depicted in Fig. 8, removing the Mamba block from our architecture, i.e., excluding the block from Fig. 4, does not significantly alter the overall performance. This suggests that the Mamba block may not be training effectively on these datasets. An alternative perspective on removing the Mamba block from EGM is to consider the GIN update equation [12]:

$$h_v^{(l)} = \mathrm{MLP}^{(l)}\left(\left(1+\epsilon^{(l)}\right)\cdot h_v^{(l-1)} + \sum\nolimits_{u\in\mathcal{N}(v)} h_u^{(l-1)}\right). \tag{19}$$

Here, l represents a GNN layer, and $(1+\epsilon^{(l)})$, with a learnable ϵ, acts as a pointwise transformation of the node embeddings. We can replace this with another `Linear` layer, making Eq. 19 analogous to learning a transformation for a node embedding via an MLP. Similarly, when the Mamba block in Fig. 4 is ablated, the EGM block performs a related set of operations:

$$h_v^{(l)} = h_v^{(l)} \oplus \mathrm{MLP}^{(l)}\left(\mathrm{MLP}^{(l)}(h_v^{(l-1)}) \oplus \sum\nolimits_{u\in\mathcal{N}(v)} h_u^{(l-1)}\right). \tag{20}$$

Here, we have replaced the $+$ symbol with $\oplus$ to emphasize the pointwise sum. This discussion indicates that the ablated EGM learns similarly to the GIN, explaining the good performance of the simplified Mamba-less model.

As to why Mamba struggles to learn effectively, we propose that treating each node as having its own sequence of states in a static graph (i.e., with a per-node sequence length of 1) contradicts Mamba's expectation of long sequences and an implementation detail that assumes the sequence length to be the fastest-changing dimension[8], thereby creating a **bottleneck**. It is unlikely that this bottleneck can be alleviated for static graphs unless we transition to operating on a sequence of nodes, similar to Graph Transformers, which, however, violates the graph inductive bias.

On the other hand, on dynamic graphs, as Table 3 illustrates, our model performs close to the state-to-the-art models, although not quite surpassing them, which is primarily a result of the model being unturned (i.e., no hyperparameter search). Moreover, as expected, the Mamba block plays an active role in the model's ability to learn on dynamic graphs, as elucidated by Fig. 9. This reinforces our prior intuition from the midway report, that dynamic graphs are more natural to train on, than static graphs, using our approach, as such graphs comprise a "sequence of graph-states". Additionally, we observe that the model was able to get good results with up to 6 blocks in the dynamic case (i.e., a deeper model on a much smaller graph), which further strengthens the notion of compatibility between learning on dynamic graphs and our approach. In the next section, we conclude this work and discuss directions for future research.

6 Conclusion & Future Work

In this report, we presented a new message-passing GNN architecture, which integrates Mamba-based State Space Models (SSMs) into Graph Neural Networks (GNNs). We began by outlining the message-passing graph neural network framework and introducing Mamba in the context of efficient long-range sequence modeling. We then suggested a formulation for incorporating Mamba into GNNs and performed several experiments to test whether our approach is viable and effective. Our proposed formulation, "Expressive Graph Mamba" (EGM), involves leveraging Mamba's SSM dynamics to facilitate message creation or node state evolution in graph-structured data, while employing standard unlearned or learned aggregation techniques for message passing between nodes. We also provided a

[8] `https://github.com/state-spaces/mamba/blob/main/mamba_ssm/ops/selective_scan_interface.py#L192`

simple extension of this model to dynamic graphs. To validate the feasibility and performance of our approach, we conducted comprehensive experiments on the Planetoid & PEMS08 datasets. Our experimental results show that the (ST)EGM model effectively learns node representations on small static & dynamic graphs. However, we struggled with scaling the EGM model on static graphs beyond a few layers, due to the training becoming increasingly unstable. This is a primary limitation of our EGM architecture, which is only partly mitigated using specific normalization schemes and skip connections, leading to stochastic training behavior, particularly for deeper networks. Furthermore, our experiments revealed that despite the incorporation of Mamba, the model's performance on static graph datasets did not demonstrate significant improvements, likely due to the sequence length bottleneck for static graphs.

Future Work We plan to expand the testing of our approach on dynamic graphs using the Temporal Graph Benchmark (TGB) [26], to more holistically evaluate the scalability and adaptability of the STEGM architecture. Additionally, we are setting up experiments on the Long Range Graph Benchmark (LRGB) [27], which consists of large graph datasets, where nodes can have long-range relationships. This might be a compatible scenario for EGM.

Another minor extension to our approach is to simplify the construction of the Mamba layer by using only the primary structured SSM equations for state updates and by decoupling the remaining layers, for example, linear projections and non-linearities, so that we can experiment with more modular architectures. The goal here would be to work around or remove the sequence length bottleneck due to the current way the Mamba block processes data. This would also allow us to examine the importance of the selection mechanism on graph-based learning tasks.

References

[1] Albert Gu and Tri Dao. Mamba: Linear-Time Sequence Modeling with Selective State Spaces. *arXiv e-prints*, art. arXiv:2312.00752, December 2023. doi: 10.48550/arXiv.2312.00752.

[2] Zhilin Yang, William W. Cohen, and Ruslan Salakhutdinov. Revisiting Semi-Supervised Learning with Graph Embeddings. *arXiv e-prints*, art. arXiv:1603.08861, March 2016. doi: 10.48550/arXiv.1603.08861.

[3] Justin Gilmer, Samuel S. Schoenholz, Patrick F. Riley, Oriol Vinyals, and George E. Dahl. Neural message passing for quantum chemistry, 2017.

[4] Pan Li and Jure Leskovec. *The Expressive Power of Graph Neural Networks*, pages 63–98. Springer Nature Singapore, Singapore, 2022. ISBN 978-981-16-6054-2. doi: 10.1007/978-981-16-6054-2_5. URL `https://doi.org/10.1007/978-981-16-6054-2_5`.

[5] Petar Veličković. Everything is connected: Graph neural networks. *Current Opinion in Structural Biology*, 79:102538, April 2023. ISSN 0959-440X. doi: 10.1016/j.sbi.2023.102538. URL `http://dx.doi.org/10.1016/j.sbi.2023.102538`.

[6] Thomas N. Kipf and Max Welling. Semi-supervised classification with graph convolutional networks. In *International Conference on Learning Representations*, 2017. URL `https://openreview.net/forum?id=SJU4ayYgl`.

[7] Yujia Li, Daniel Tarlow, Marc Brockschmidt, and Richard S. Zemel. Gated graph sequence neural networks. In Yoshua Bengio and Yann LeCun, editors, *4th International Conference on Learning Representations, ICLR 2016, San Juan, Puerto Rico, May 2-4, 2016, Conference Track Proceedings*, 2016. URL `http://arxiv.org/abs/1511.05493`.

[8] William L. Hamilton, Rex Ying, and Jure Leskovec. Inductive representation learning on large graphs. In *Proceedings of the 31st International Conference on Neural Information Processing Systems*, NIPS'17, page 1025–1035, Red Hook, NY, USA, 2017. Curran Associates Inc. ISBN 9781510860964.

[9] Petar Veličković, Guillem Cucurull, Arantxa Casanova, Adriana Romero, Pietro Liò, and Yoshua Bengio. Graph attention networks. In *International Conference on Learning Representations*, 2018. URL `https://openreview.net/forum?id=rJXMpikCZ`.

[10] Shaked Brody, Uri Alon, and Eran Yahav. How attentive are graph attention networks? In *International Conference on Learning Representations*, 2022. URL `https://openreview.net/forum?id=F72ximsx7C1`.

[11] Seongjun Yun, Minbyul Jeong, Raehyun Kim, Jaewoo Kang, and Hyunwoo J Kim. Graph transformer networks. In *Advances in Neural Information Processing Systems*, pages 11960–11970, 2019.

[12] Keyulu Xu, Weihua Hu, Jure Leskovec, and Stefanie Jegelka. How powerful are graph neural networks? In *International Conference on Learning Representations*, 2019. URL `https://openreview.net/forum?id=ryGs6iA5Km`.

[13] Bing Yu, Haoteng Yin, and Zhanxing Zhu. Spatio-temporal graph convolutional networks: A deep learning framework for traffic forecasting. In *Proceedings of the 27th International Joint Conference on Artificial Intelligence (IJCAI)*, 2018.

[14] Yaguang Li, Rose Yu, Cyrus Shahabi, and Yan Liu. Diffusion convolutional recurrent neural network: Data-driven traffic forecasting. In *International Conference on Learning Representations*, 2018. URL `https://openreview.net/forum?id=SJiHXGWAZ`.

[15] Zonghan Wu, Shirui Pan, Guodong Long, Jing Jiang, and Chengqi Zhang. Graph wavenet for deep spatial-temporal graph modeling. In *Proceedings of the Twenty-Eighth International Joint Conference on Artificial Intelligence, IJCAI-19*, pages 1907–1913. International Joint Conferences on Artificial Intelligence Organization, 7 2019. doi: 10.24963/ijcai.2019/264. URL `https://doi.org/10.24963/ijcai.2019/264`.

[16] Chao Song, Youfang Lin, Shengnan Guo, and Huaiyu Wan. Spatial-temporal synchronous graph convolutional networks: A new framework for spatial-temporal network data forecasting. *Proceedings of the AAAI Conference on Artificial Intelligence*, 34(01):914–921, Apr. 2020. doi: 10.1609/aaai.v34i01.5438. URL `https://ojs.aaai.org/index.php/AAAI/article/view/5438`.

[17] Lei Bai, Lina Yao, Can Li, Xianzhi Wang, and Can Wang. Adaptive graph convolutional recurrent network for traffic forecasting, 2020.

[18] Yuchen Fang, Yanjun Qin, Haiyong Luo, Fang Zhao, Bingbing Xu, Liang Zeng, and Chenxing Wang. When spatio-temporal meet wavelets: Disentangled traffic forecasting via efficient spectral graph attention networks. In *2023 IEEE 39th International Conference on Data Engineering (ICDE)*, pages 517–529, 2023. doi: 10.1109/ICDE55515.2023.00046.

[19] Hangchen Liu, Zheng Dong, Renhe Jiang, Jiewen Deng, Jinliang Deng, Quanjun Chen, and Xuan Song. Spatio-temporal adaptive embedding makes vanilla transformer sota for traffic forecasting. In *Proceedings of the 32nd ACM International Conference on Information and Knowledge Management*, CIKM '23, page 4125–4129, New York, NY, USA, 2023. Association for Computing Machinery. ISBN 9798400701245. doi: 10.1145/3583780.3615160. URL `https://doi.org/10.1145/3583780.3615160`.

[20] Albert Gu, Tri Dao, Stefano Ermon, Atri Rudra, and Christopher Ré. Hippo: Recurrent memory with optimal polynomial projections. *CoRR*, abs/2008.07669, 2020. URL `https://arxiv.org/abs/2008.07669`.

[21] Jimmy Lei Ba, Jamie Ryan Kiros, and Geoffrey E. Hinton. Layer normalization, 2016.

[22] Peter J. Huber. Robust Estimation of a Location Parameter. *The Annals of Mathematical Statistics*, 35(1):73 – 101, 1964. doi: 10.1214/aoms/1177703732. URL `https://doi.org/10.1214/aoms/1177703732`.

[23] Liyuan Liu, Haoming Jiang, Pengcheng He, Weizhu Chen, Xiaodong Liu, Jianfeng Gao, and Jiawei Han. On the variance of the adaptive learning rate and beyond. In *International Conference on Learning Representations*, 2020. URL `https://openreview.net/forum?id=rkgz2aEKDr`.

[24] Biao Zhang and Rico Sennrich. Root mean square layer normalization, 2019.

[25] Takeru Miyato, Toshiki Kataoka, Masanori Koyama, and Yuichi Yoshida. Spectral normalization for generative adversarial networks. In *International Conference on Learning Representations*, 2018. URL `https://openreview.net/forum?id=B1QRgziT-`.

[26] Shenyang Huang, Farimah Poursafaei, Jacob Danovitch, Matthias Fey, Weihua Hu, Emanuele Rossi, Jure Leskovec, Michael Bronstein, Guillaume Rabusseau, and Reihaneh Rabbany. Temporal graph benchmark for machine learning on temporal graphs. *Advances in Neural Information Processing Systems*, 2023.

[27] Vijay Prakash Dwivedi, Ladislav Rampášek, Mikhail Galkin, Ali Parviz, Guy Wolf, Anh Tuan Luu, and Dominique Beaini. Long range graph benchmark. In *Thirty-sixth Conference on Neural Information Processing Systems Datasets and Benchmarks Track*, 2022. URL `https://openreview.net/forum?id=in7XC5RcjEn`.